

k_La measurement in bioreactors

F. Scargiali, A. Busciglio, F. Grisafi, A. Brucato

Dip. di Ingegneria Chimica, dei Processi e dei Materiali, Università di Palermo

Viale delle Scienze, Ed. 6, 90128, Palermo, Italy

For accurately measuring k_La in bioreactors the *dynamic pressure method* (DPM) was introduced by Linek *et al.* (1993). In this work a simplified version of the same method is discussed. With respect to the original DPM, the simplified version greatly simplifies data treatment. In fact final constant slope observable in the usual semi-log diagram of residual driving force versus time may be simply corrected to obtain the real k_La value with negligible inaccuracy.

Experimental data obtained on a lab-size stirred tank reactor confirm all model predictions, including the feature that the adoption of large pressure changes may lead to a better accuracy.

1. Mathematical modeling

In the DPM, the driving force for oxygen absorption is obtained by means of small operating pressure step-changes in the vessel (Linek *et al.*, 1989, Linek *et al.*, 1993, Moucha *et al.*, 1995, Fujasova *et al.*, 2007). For instance, vacuum may be applied to the system and, after sufficient oxygen depletion is attained, atmospheric pressure is suddenly restored by admitting atmospheric air to the reactor head-space. Air might be considered as if it was a single component gas. The subsequent system transient would therefore be described as if it involved only the absorption of this pseudo-component, until saturation. Measured oxygen transient concentrations up to saturation might be regarded as mimicking the single component concentration evolution. This however does not exactly coincide with what actually occurs in gas-liquid dispersions, as the simultaneous presence of at least two different components (oxygen and nitrogen, each one characterized by its own solubility and diffusivity) must be accounted for. The fundamental equations involved are the mass balances in both liquid and gas phases, that in the following simplified model will be assumed to be perfectly mixed;

$$\frac{dC_{LO_2}}{dt} = N_{O_2} \quad (1)$$

$$\frac{dC_{LN_2}}{dt} = N_{N_2} \quad (2)$$

$$\frac{dM_{g,O_2}}{dt} = F_{O_2,in} - F_{O_2,out} - V_L N_{O_2} \quad (3)$$

$$\frac{dM_{g,N_2}}{dt} = F_{N_2,in} - F_{N_2,out} - V_L N_{N_2} \quad (4)$$

Where C, and M are liquid concentration and component mass in the gas phase respectively. The gas rate leaving the dispersion is modelled as being proportional to gas hold-up ε and average bubble rise velocity u_t ,

$$F_{g,out} = S u_t \varepsilon \frac{P}{RT} \quad (5)$$

Where S is tank transversal section and P is system pressure. The oxygen and nitrogen interfacial flow rates per unit dispersion volume are computed as:

$$N_{O_2} = k_{LO_2} a (C_{LO_2}^* - C_{LO_2}) \quad (6)$$

$$N_{N_2} = k_{LN_2} a (C_{LN_2}^* - C_{LN_2}) \quad (7)$$

According to the penetration theory, the transport coefficients of oxygen and nitrogen are assumed to be linked by the following expression;

$$\frac{k_{LN_2}}{k_{LO_2}} = \sqrt{\frac{D_{N_2}}{D_{O_2}}} \quad (8)$$

This simple set of equations was numerically solved for simulating the liquid and gas concentration transients following a sudden pressure change in the system. To this end, a value of $k_{L,O_2} a$ (hereafter referred to as $k_L a$) was specified. As the pressure variation compresses the bubbles, it gives rise to a sudden decrease in phase concentration and volumetric hold-up, so that also these quantities undergo a transient that was also simulated. Typical results are shown in Fig. 1 a and b.

Despite these disturbances, the oxygen and nitrogen dynamics show a quite regular increase as shown in Fig.2 and, when their residual driving forces are plotted vs time in a *semi-log* diagram, they give rise to fairly straight lines, as it can be appreciated in Fig. 3. It is worth noting however that none of the two constant slopes observable in the same figure does coincide with the known $-k_L a$ value (imposed as model parameter).

By comparing the observed oxygen slope vs input $k_L a$, it can be seen that for small enough $k_L a$ values a negligible difference, smaller than (1 – 2 %) exists between the two. This implies that for small enough $k_L a$ values (e.g $k_L a < 0.03s^{-1}$) the dynamic technique may be employed just as if a pure gas were absorbed in a previously evacuated liquid.

For larger $k_L a$ values, the discrepancy increases and the simple slope detection in Fig. 3 would lead to unacceptably large errors.

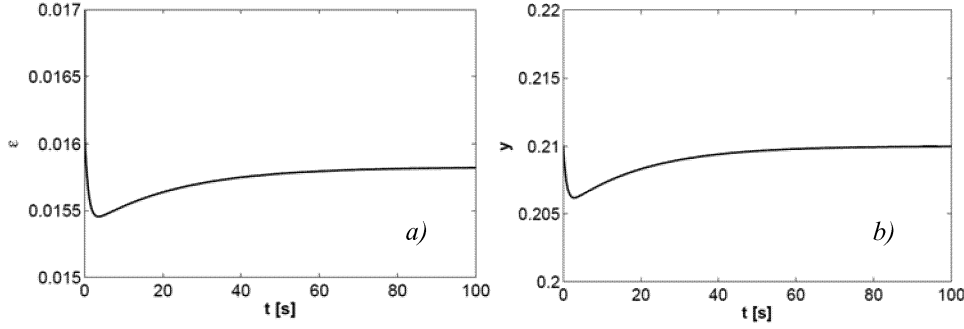


Fig. 1: Simulated hold-up (a) and gas phase composition (b) dynamics for $k_L a = 0.05 s^{-1}$, $Q_g = 1 vvm$, $P_0 = 0.5 atm$, $P_{final} = 1 atm$

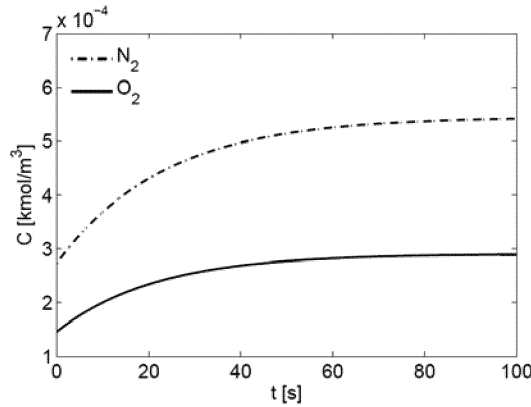


Fig. 2: Liquid phase simulated Oxygen and Nitrogen dynamics

In an attempt to understand why under such conditions straight lines are still obtained (though with slopes not exactly coinciding with $-k_L a$), the further assumption that gas phase mass variations with time are negligible may be added to the previous model hypotheses. Under this additional hypothesis $F_{out} \sim F_{in}$ and the liquid phase oxygen balance can be manipulated to give:

$$\frac{dC_{LO_2}}{C_{LO_2}^* - C_{LO_2}} = \frac{k_L a}{1 - k_L a \frac{V_L \text{Sol}_{O_2}}{F_{in}}} dt \quad (9)$$

which implies that the O_2 driving force line in Fig. 3 should actually be expected to result in a straight line with a slope given by:

$$\text{Slope} = \frac{k_L a}{1 - k_L a \frac{V_L \text{Sol}_{O_2}}{F_{in}}} \quad (10)$$

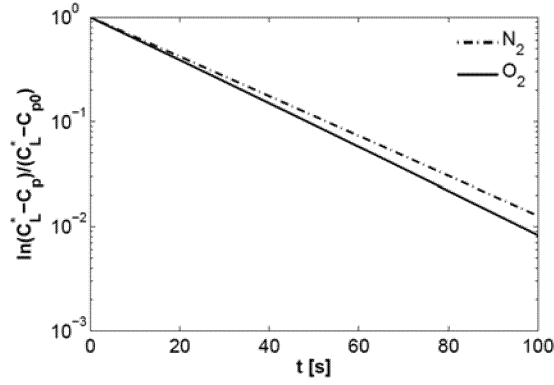


Fig. 3: Simulated liquid phase concentration dynamics for $k_L a = 0.05 s^{-1}$, $Q_g = 1 vvm$, $P_0 = 0.5 atm$, $P_{final} = 1 atm$

hence a slope different from $k_L a$. This last can however be easily obtained from Eqn. 10. Eqn. 10 was tested against many model simulations concerning widely varying $k_L a$ values. Results showed that the correction provided by Eqn. 10 tends to over-correct the experimental slopes, probably because, under the above additional hypothesis, no role is left in the model equations to nitrogen solubility and diffusivity. By suitably modifying Eqn. 10 on the basis of observed discrepancies, the following more effective correction was obtained:

$$k_L a = -\text{Slope} \frac{1 + \text{Slope} \frac{V_L \text{Sol}_{N_2}}{F_{in}} \sqrt{\frac{D_{O_2}}{D_{N_2}}}}{1 + \text{Slope} \frac{V_L \text{Sol}_{O_2}}{F_{in}}} \quad (11)$$

With this correction the errors incurred in the evaluation of $k_L a$ on the basis of the observed oxygen dynamics slopes are well acceptable, being always much smaller than 2 %.

Summarizing, a simplified version (SDPM) of the DPM may be proposed, in which oxygen dynamics data analysis is simply done by (i) plotting the residual driving force on a *semi-log* diagram, (ii) assessing the final slope value and (iii) employing Eqn. 11 to obtain the relevant $k_L a$ value.

Notably, the observed slopes were found to be practically independent of pressure increase extent, a feature with important practical implications as larger pressure changes result into larger residual driving forces, so making for easier and more accurate measurements.

The simplified version of the DPM here proposed is somewhat less accurate than the original technique introduced by Linek *et al.*, (1993), but has the advantage of being much more straightforward by substantially getting away with the computational burden of the original method, at the expense of inaccuracies smaller than experimental uncertainties.

2. Application to standard geometry bioreactors

Experimental measurements were carried out on the standard stirred reactor described in Scargiali *et al* (2010). For comparison purposes, $k_L a$ measurements were also performed via the well established OApE procedure and the more common OAS procedure (Scargiali *et al*, 2007).

As concerns the model prediction that the ΔP extent should not significantly affect the results, in Fig.4 results obtained in three runs conducted with three widely differing pressure changes (from 25% to as much as 900%, on initial pressure basis) are reported for two different operating conditions. As it can be seen in all cases practically the same final constant slope is observed, irrespectively of the pressure change extent, fully confirming model predictions. This has interesting practical implications as the adoption of larger pressure changes simplifies the assessment of oxygen concentration differences with respect to final equilibrium conditions.

All SDPM experimental results obtained under 1 vvm gassing rate and various agitation speeds are reported in Fig. 5 vs the relevant real values obtained with the OApE technique.

As it can be seen, measurements obtained with SDPM do practically coincide with those obtained with the OApE technique, hence further validating the SDPM.

The data obtained in this work were finally correlated by the usual power law expression. Correlation parameters were assessed *via* bivariate non-linear regression applied to all experimental data obtained, resulting in the following correlation with an R squared of 0.996:

$$k_L a = 0.0037 v_s^{0.35} \left(\frac{P_g}{V_L} \right)^{0.59} \quad (4)$$

In Fig. 5 the experimental $k_L a$ values divided by the 0.35 power of superficial gas velocity are plotted vs specific power input in a *log-log* diagram and, as it can be seen, the data are found to line up on a single straight line with a slope of 0.58.

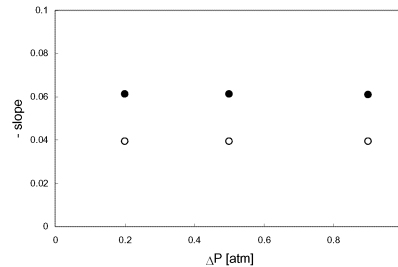


Fig. 4: Observed “-slope” exp. obtained at various pressure increase extent at 900 (open symb) and 1100 rpm (full symb).

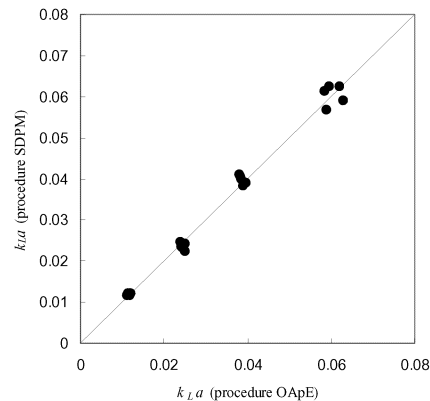


Fig. 5: Comparison between $k_L a$ values determined with the three variants of the dynamic method at various agitation speeds

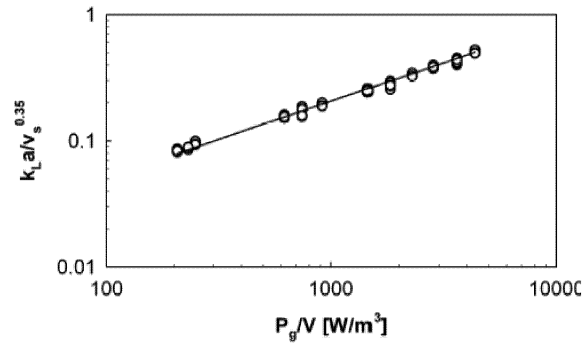


Fig. 6: $k_L a / v_s^{0.35}$ vs P_g / V_L . Symbols: experimental data; continuous line: Eqn. 4.

3. Conclusions

A simplified version of the DPM for measuring mass-transfer coefficients in gas-liquid systems was proposed. Experimental validation showed that SDPM is a viable procedure that gives rise to results practically coinciding with the real $k_L a$ values obtained in the absence of nitrogen.

Notation

a : gas-liquid interfacial area per unit vol. [m^2];	R : gas universal constant [$Pa\ m^3\ kmol^{-1}\ K^{-1}$];
C_L : oxygen conc. in the liquid phase [$kmol\ m^{-3}$];	S : tank transversal section [m^2];
C_L^* : overall equilibrium oxygen conc. [$kmol\ m^{-3}$];	$Sol_{N_2} = (1-y) (p\ C_{Tot,L}) / H_{N_2}$ [$kmol\ m^{-3}$];
D : gas diffusivity [$m^2\ s^{-1}$];	$Sol_{O_2} = y (p\ C_{Tot,L}) / H_{O_2}$ [$kmol\ m^{-3}$];
F : molar gas flow-rate [$kmol\ s^{-1}$];	T : system temperature [K];
H_{N_2} : Henry's constant for Nitrogen [Pa]	u_t : average bubble terminal rise velocity [$m\ s^{-1}$];
H_{O_2} : Henry's constant for Oxygen [Pa]	V_L : liquid volume [m^3];
k_L, k_{L,O_2} : oxygen mass transfer coefficient [$m\ s^{-1}$];	v_s : superficial gas velocity [$m\ s^{-1}$];
k_{L,N_2} : nitrogen mass transfer coefficient [$m\ s^{-1}$];	DPM: Dynamic Pressure Method;
Mg : overall mole number in the gas phase [$kmol$];	OApE: pure Oxygen Abs. in Pre-Evac. water;
P : system pressure [Pa]	OAS: pure Oxygen Abs. in Air Sat. water;
Pg/V : specific gassed power input [$W\ m^{-3}$];	SDPM: Simplified Dynamic Pressure Method;

References

- M. Fugasova, V. Linek, T. Moucha, 2007, *Chem. Eng. Sci.* 62, 1650-1669.
 V. Linek, P. Vacek, P. Benes, 1987, *Chem. Eng. J.*, 4, 1-34.
 V. Linek, P. Benes, P. Vacek, 1989, 33, 1406-1412.
 V. Linek, P. Benes, J. Sinkule, T. Moucha, 1993, *Chem. Eng. Sci.* 48(9), 1593-1599.
 T. Moucha, V. Linek, J. Sinkule, 1995, *Trans. I.Chem.Eng.* 73A, 286-290.
 R. Perry, D. Green, Perry's Chemical Engineers' Handbook, 8th ed., McGraw - Hill, Int., 2008
 F. Scargiali, R. Russo, F. Grisafi, A. Brucato, 2007, *Chem. Eng. Sci.* 62, 1376-1387.
 F. Scargiali, A. Busciglio, F. Grisafi, A. Brucato, 2010, *Biochem. Eng. J.*